JOURNAL OF SOLID STATE CHEMISTRY 88, 53–69 (1990)

Pure and Doped Vanadium Sesquioxide: A Brief Experimental Review

MOHANA YETHIRAJ

Manuel Lujan, Jr. Neutron Scattering Center, P-LANSCE, MS H805, Los Alamos National Laboratory, Los Alamos, New Mexico

Received April 2, 1990

DEDICATED TO J. M. HONIG ON THE OCCASION OF HIS 65TH BIRTHDAY

Vanadium sesquioxide (V_2O_3) undergoes a number of phase transitions as a function of temperature and doping. These phase transformations have been studied extensively using numerous experimental techniques. In this article, I shall attempt to briefly review the experimental data on the pure and doped V_2O_3 system. © 1990 Academic Press, Inc.

Introduction

The metal–insulator phase transitions in vanadium sesquioxide have been extensively studied for over four decades and hundreds of papers on this topic have been published (*1*). Metal–insulator transitions and phase transitions, in general, have always been a subject of great interest, both experimentally and theoretically, because the knowledge of mechanisms driving these transformations lends a great deal of insight into the nature of forces in play. While it may be a theoretical challenge to explain the properties of any given phase, the successful theory of a phase transition must not only identify the transition mechanism that drive the changes, but must also simultaneously determine the physical properties of both the phases involved. Although transitions exist in several 3*d* metal oxides, the particular fascination with the V_2O_3 system is by no means unjustified. Vanadium sesquioxide (V_2O_3) along with its chromium and titanium doped cousins form a class of compounds that manifests a number of phase transitions as a function of temperature, dopant content, and pressure.

Even though these phase changes are intriguing in themselves, the fact that this metal–insulator transition was thought to be an example of a Mott transition gave this research added impetus. In 1946, even preceding the Mott theory, the first-order metal–insulator transition was observed (*2*) in V_2O_3 as the temperature was lowered below approximately 160 K. Mott initially advanced the theory (*3*) of this transition in 1952 and showed that, as the distance between the atoms in a lattice was increased, it would be possible for a metal to transform to an insulator, perhaps simultaneous with the onset of magnetic order. Although the above explanation is extremely simplified, it will suffice to show clearly the motivation for several experimental studies that were undertaken.

By 1970, there was a large body of experi-

0022-4596/90 $3.00

mental work which started off a very active debate as to the transition mechanisms, even though a detailed microscopic picture of the Mott theory still did not exist. It was about this time that V_2O_3 began to be doped with other 3*d* transition metals in order to cause variations in the lattice parameters and serve as a test of the theory. It was found, in one of the attempts to vary lattice parameters, that the low temperature insulating phase of V_2O_3 could be entirely suppressed (*4*) by the application of pressures greater than 26 kbar. The experimentation with doping also turned out to be extremely fruitful. Researchers at Bell Laboratories and elsewhere showed conclusively that the Ti-doped (*5*) or O-rich (*6*) samples behaved exactly as pure V_2O_3 specimens to which hydrostatic pressure was applied. In addition, they were also able to show that chromium doping acted as a negative pressure on the lattice, although the addition of Cr causes the lattice to expand nonisotropically. However, the effects of doping on the phase transitions were much more complex than expected and has led to a continuing experimental effort on this problem.

The first resistivity measurements (*2, 7*) were accompanied by other traditional methods of investigation of phase transitions, including specific heat (*8*) measurements. These initial measurements have since been repeated and, with better characterized samples now available, a consistent picture has emerged. Further, as more modern experimental techniques such as ultrasound, neutron scattering, and NMR, to name just a few, became routine, these too were used to study the properties of the different phases in the V_2O_3 system. Detailed quantitative measurements of lattice dynamical, thermodynamical, structural, and magnetic properties in the pure and doped V_2O_3 system now exist and the primary object of this article is to review, albeit briefly, the salient features in the profusion of experimental information on pure, chromium-doped and titanium-doped V_2O_3 that has been published thus far.

In the meanwhile, several theories (*9–11*) have been put forward to explain the many experimental facts that had been determined. It is not in the scope of this article to fully address these theories and they are reviewed elsewhere (*12*). It is enough to say that, although progress has been made in explaining the phase diagram (*12a*), the description of the driving forces encompassing all the transitions observed in these materials is yet incomplete.

In the following section, I outline the phase diagram of pure and doped V_2O_3 as a function of temperature and dopant content. In the next sections, I discuss the transport phenomena, the structural and lattice dynamical properties, the magnetic properties, and the electron band properties, and how these are affected by Cr-doping as well as by Ti-doping and by departure from exact stoichiometry. In the last section, I attempt to make some conclusions about how these results pertain to any theoretical approach.

Phase Diagram for Pure and Doped V_2O_3

The widely accepted phase diagram (*13*) as a function of temperature and dopant concentration is shown in Fig. 1. Pure V_2O_3 is represented by the line at $x = 0$. To explain the phase diagram, this section will concentrate primarily on the gross properties of this system, using the resistivity measurements as a guide.

The low temperature metal–insulator transition in pure V_2O_3 is accompanied by a simultaneous change in the structure from trigonal to monoclinic (*14*) and onset of long-range antiferromagnetic (*15*) order. A trigonal cell can be uniquely described by *c* and *a* lattice parameters with the commonly used hexagonal indexing. To simplify the structural comparisons, the monoclinic distortion is sometimes ignored and this phase is indexed "pseudo-hexagonally."

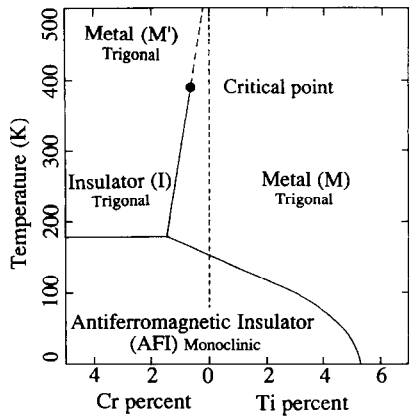

FIG. 1. The phase diagram for V_2O_3 as a function of temperature and dopant content. The dashed line represents pure V_2O_3. Ti and Cr doping has the effect of positive and negative pressure, respectively. 1% dopant corresponds approximately to 4 kbar. (From Ref. (*41*).)

Doping with Cr leads to the formation (*16*) of a new insulating phase that is not seen in the pure compound. On the other hand, addition of Ti or excess O content serves to stabilize the metallic phase (*5, 6*) at the expense of the low temperature insulating phase. This can be seen in the phase diagram and is also detailed in this section.

(*a*) *Pure* V_2O_3

V_2O_3 undergoes a first-order metal–insulator transition as a function of temperature, at approximately 160 K. First reported by Foex (*2*) this transition has since been reexamined on numerous occasions (*2, 7, 17, 18*). As the temperature is raised above ~160 K, the resistivity of good single crystal specimens has been seen to decrease by as much as eight orders of magnitude, as shown in Fig. 2. At this temperature, the monoclinic structure changes to a higher symmetry trigonal cell (*14, 19*) and, simultaneously, the ordered magnetism disappears (*15, 20*).

After considerable initial dispute between interpretations of the first NMR (*21, 22*), Mössbauer (*23*), and neutron scattering (*24*) data, polarized neutron scattering results (*15, 20*) conclusively showed that the low-temperature insulating phase was antiferromagnetic; from now on it is referred to as the antiferromagnetic insulating (or AFI) phase. The magnetic moment per V atom is 1.2 μ_B and the moments lie perpendicular to the hexagonal a-axis and ~71° from the hexagonal c-axis. The arrangement is such that c–a planes with spins aligned in the same direction are stacked antiferromagnetically along the $(110)_H$ axis.

The room temperature metallic (M) phase was determined to be isostructural with α-Al_2O_3 (corundum). This trigonal structure was shown by Dernier and Marezio (*19*) to transform to a monoclinic symmetry as the material was cooled below the transition. Each of the $(110)_H$ axes in the hexagonally indexed trigonal cell becomes an unique $(010)_M$ axis in the monoclinic cell. Since

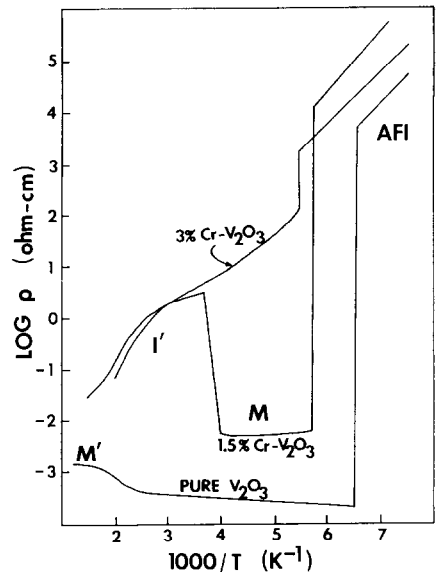

FIG. 2. The plot of resistivity versus reciprocal temperature for a few representative Cr-doped compounds clearly show the various transitions that can exist as a function of temperature and dopant content. (From Ref. (*18*).)

there are three equivalent $(110)_H$ directions in the trigonal cell, three unique but spacially related monoclinic domains are seen to exist in the low temperature insulating phase of V_2O_3. In other words, the monoclinic cell exhibits a triple twinning.

As the temperature is raised above approximately 550 K, the resistivity shows a gradual increase indicating a second transformation to another metallic (M′) phase. This change from M to M′ exhibits no change of the trigonal symmetry and neither of the metallic phases has any long-range magnetic order.

In short, V_2O_3 can be characterized by three behavioral regimes. At the lowest temperatures, the material is stable in (i) the AFI monoclinic phase which transforms to (ii) the trigonal M phase at ~160 K, which then further undergoes a change to (iii) a second metallic M′ phase with no change in lattice symmetry at ~550 K.

(b) Doped and Nonstoichiometric V_2O_3

The addition of small amounts of chromium to V_2O_3 effects dramatic differences (*25*) in the electrical properties of the compound. Although, at the lowest temperatures, $(Cr_xV_{1-x})_2O_3$, for up to $x \sim 0.30$, is seen to be monoclinic and has the same magnetic arrangement of moments as the undoped compound, even a small percentage of Cr has a large effect on the phase decision between 160 and 500 K, as can be seen in Fig. 2.

For samples with $0.005 < x < 0.03$, raising the temperature above ~160 K induces the transition from AFI to the M phase, as in pure V_2O_3. In this range, as the dopant level is increased, the temperature of the discontinuity in resistivity increases while the magnitude of this anomaly decreases. On further warming, there is a transition to a second insulating phase (I) that is nonmagnetic. The temperature of this M–I change depends on the Cr concentration. For example, in samples

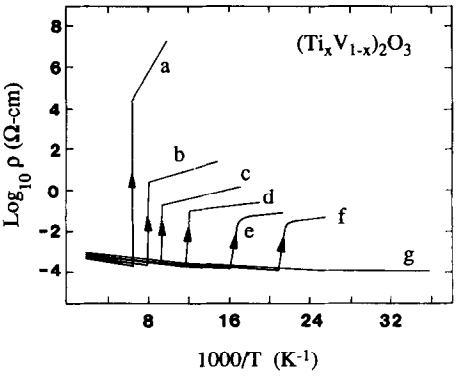

FIG. 3. The resistivity curves for $(Ti_xV_{1-x})_2O_3$ compounds for x = 0.0, 1.0, 2.0, 3.0, 4.0, 4.9, and 5.5%, respectively. The size of the anomaly as well as the slope in the AFI phase decrease with increase in the Ti dopant levels. (From Ref. (*30*).)

with $x = 0.015$, this transformation occurs at about room temperature. This sharpness of this transformation has been of some debate (*26, 27*), and it is now agreed (*28*) that this resistance change occurs in many discrete steps. Rise in temperature above this M–I transition results in a monotonic decrease in resistivity that approaches the resistivity of pure V_2O_3 at the highest temperature measured (~800 K).

In $(Cr_xV_{1-x})_2O_3$ specimens with $x > 0.02$, there is a drop in resistivity at approximately 175 K of only one order of magnitude and the system goes directly from the AFI to the I phase and the M state does not appear. Above 400 K, the resistivity curve of 3% Cr-doped samples follows that of those Cr-doped samples that underwent M–I transitions at lower temperatures. In Cr-doped samples with $x < .005$, there is no clear discontinuity in resistivity at about ~400 K, and it is suggested (*6, 25*) that the M–I transition as a function of Cr-doping ends in a critical point. This would indicate that the increase in resistivity in pure V_2O_3 (the *M–M′* change) is simply a manifestation of supercritical behavior.

On the other hand, using titanium as a

dopant affects the AFI–M transition temperature, T_{M-AFI} as well. As x in $(Ti_x V_{1-x})_2O_3$ is increased, the temperature of the phase change to the AFI state is depressed and for $x > 0.055$, the M phase is stabilized to the lowest temperatures and the AFI phase is entirely suppressed (*29, 30*). Also, as T_{M-AFI} decreases, the size of the jump in resistivity also decreases. (See Fig. 3).

Departure from stoichiometry (oxygen excess or metal-deficiency) in V_2O_3 samples also causes the M–AFI phase transition to occur (*31, 32*) at lower temperatures. Similar to Ti-doped samples, in V_2O_{3+x} samples, no transition occurs for values of $x > 0.03$; the difference is that the size of the resistivity discontinuity is larger when the transition temperature is depressed.

Structurally, the AFI phase uniformly has a monoclinic unit cell. All the other (M, I, and M′) phases have a trigonal lattice symmetry, whether the dopant is Cr or Ti or vacancies. None of these trigonal phases exhibits long-range magnetic order.

It is important to note (*33*) that the doped samples are homogeneous. The effects that are seen in the resistivity and other data are not due to merely a macroscopic mixing of the dopant and the host material. In Cr- and Ti-doped samples, it is generally believed that the dopant atoms go in substitutionally for V atoms since there has been no observation of superlattice peaks in neutron and X-ray scattering studies. Nonstoichiometric samples are, strictly speaking, metal-deficient and not oxygen-rich (*34*) since the departure from stoichiometry is attained by a partial occupancy of the metal sites. The oxygen sites are fully occupied in stoichiometric specimens. It is perhaps interesting to note here that the quality of samples used in past work can be gauged for deterioration via oxidation by the transition temperature that is reported, since this temperature is so sensitive to the oxygen stoichiometry.

Physical Properties of the Pure and Doped V_2O_3 System

(*a*) *Transport Properties*

The measurements outlined above provided the first evidence for the metal–insulator transition in V_2O_3. Careful analyses of the resistance data (*35*) provide even more information about the properties of the different phases. In this section, the anomalous resistance properties as well as the data on specific heat and entropy changes will be reviewed.

In the AFI phase, the resistivity has a negative temperature coefficient, as can be seen from Fig. 1. Log (ρ) is proportional to the reciprocal temperature, the slope indicating an activation energy of approximately 0.1 eV. At the transition to the M phase, in samples where the M phase exists, there is a large discontinuity in the resistance. For Cr-doped samples in the AFI phase, ρ increases with dopant level of up to 3%, but drops again for samples that do not undergo the AFI–M change.

There are a number of resistance anomalies in the M phase. To study the M phase in greater detail, experiments have also been carried out where the AFI phase was completely suppressed by application of pressure greater than 26 kbar. In this phase, the resistivity is seen to have a positive temperature coefficient prior to the steeper rise connected with the change to the M′ phase. In addition, it was found (*4*) that, in this pressure-stabilized M phase,the contribution to the resistivity that is proportional to T^2, saturating at ~100 K, is much larger than in other metal oxides or metals. Originally ascribed to electron–electron or electron-hole scattering, this T^2 term has also been interpreted as being due to spin fluctuations, which would be expected to play a noticeable role at the low temperatures. In fact, in the theory proposed by Hertel and Appel (*36*) using a Fermi liquid model involving antiferromagnetic spin fluctuations, several

properties of the M phase can be explained. Cr-doping is seen to correspond to an increased ρ in the M phase. It is possible that this is due to "impurity" scattering due to the dopant itself, but it is more probable that the M phase in $(Cr_xV_{1-x})_2O_3$ actually consists of the coexistence (in varying degrees) of both the M and I states, as structural and magnetic evidence, discussed later, will indicate.

The M phase in this system has a resistivity that is somewhat high for a "true" metal, about two orders of magnitude greater, for instance, than copper. This together with the fact that the Seebeck coefficient (*37, 38*) of V_2O_3 in the M phase is also rather high (measured values of a range from $+3$ to $+15$ μV/°) suggest that the M phase is in fact semimetallic rather than metallic.

It has been pointed out (*4*) that the temperature ~700 K that drives the system into the M′ phase is of the order of the activation energy seen in the AFI phase and that, with this in view, the resistivity decrease at the M′ phase is governed primarily by carrier mobility rather than carrier activation. This was postulated as being the main difference between the I and M′ phases.

The electrical properties of $(Ti_xV_{1-x})_2O_3$ and $V_2O_{3+\delta}$ have also been documented. Shivashankar and Honig, in a quantitative study (*30*) of these features, found that, in qualitative agreement with previous (*28, 39, 40*) reports, doping with Ti or increasing the oxygen content does lower the M–AFI transition temperature and that this transition is completely bypassed for x (Ti content) > 0.055 or for δ (oxygen excess) ~0.03. In addition, the resistivity activation energy (i.e., the slope of log ρ versus reciprocal temperature) in the AFI phase also diminishes as x or δ is increased. The size of the ρ discontinuity, however, increases for O-rich specimens but decreases for Ti-doped samples. This jump is observed to be more than 11 orders of magnitude for δ ~0.025. These features have been semiquantitatively explained on the basis that acoustic lattice vibrations are the primary scattering mechanism in $(Ti_xV_{1-x})_2O_3$ and that ionized impurity scattering dominates in $V_2O_{3+\delta}$. This analysis made the assumption that having Ti as a dopant or V vacancies introduces acceptor centers in the material, making the host material more extrinsic and hence causing the Fermi level to move closer to the valence band edge. This is consistent with the fact that the activation energy is reduced as the dopant level is increased.

In thermodynamic measurements, which looks at a different aspect of the phase transition, the Bell Laboratories group (*41*) found an anomalously large linear contribution to the specific heat in the M phase of V_2O_3, where it exists in Ti-doped, O-rich, and pressure-induced samples. This has been interpreted as being due to electron–electron interactions. It should be mentioned here that it is not impossible that this contribution is due to electron–phonon effects. In this context, it should be mentioned, as several researchers have noted, that transitions involving the M phase always appear to have large hysterises, possibly due to the sluggishness of the lattice.

In more detailed calorimetry work, researchers have reported (*42*) on the entropy change at phase transitions in both pure and Cr-doped samples. It has been seen that the change in entropy, ΔS, at the AFI–M is smaller than the ΔS calculated due to the onset of magnetic ordering alone, even assuming that only one of the two V atoms contributes to the ordering. The measured entropy of the M phase in pure V_2O_3 is larger than in the AFI phase by 11.2 J/mole-K. Similarly, for $x = 0.015$ and 0.030, the ΔS at the magnetic transition is measured to be 12.3 and 10.9 J/mole-K, respectively, also smaller than the calculated magnetic contribution by about 15%. Further, because the magnetic moment is not saturated just below the transition temperature, even in the pure compound, the calculated value may well

be overestimated. It has also been pointed out that the measured (*43*) spin-wave gap of 4.75 meV has not been taken into account, although no specific heat anomaly associated with the spin-wave gap temperature of 50–60 K has been reported. Even so, this measurement of the change in entropy would appear to indicate that the magnetic component of the transition is the most important feature of the transformation to the AFI phase.

Measurements of the entropy change have also been made for the high temperature transitions. Here, it is seen that the entropy of the I phase is smaller than that of the M phase. Reports conflict as to the change in entropy at the transformation to the M' phase, measured values vary from 0 (*44*, *45*) to 0.3 J/mole-K (*46*). The zero value for ΔS has been interpreted as evidence against a phase transition in the thermodynamic sense. The I′–M′ transformation appears to be very sluggish and spread over a wide temperature interval, however, and this may account for the lack of any significant change in measured entropy in a differential calorimetry scan at any given temperature.

(*b*) *Crystallographic and Lattice Properties*

The high temperature (M′, M, and I) phases of pure and doped V_2O_3 have a trigonal $R3c$ lattice symmetry, similar to other metal sesquioxides such as α-Al_2O_3 (corundum), Fe_2O_3, Ti_2O_3, and Cr_2O_3 and, initially, there appears to be nothing unusual about the crystal structure of V_2O_3. However, closer examination of pure V_2O_3 at room temperature showed (*13*) that the M phase exhibits an anomalously large c/a ratio in comparison to the other metal oxides that share the same symmetry. This ratio for the pure V_2O_3 specimen in the M phase is 2.82, about 4% larger than in corundum, for instance. The compressibility (*47*, *48*) of vanadium sesquioxide is also more anisotropic. Whereas, for Cr_2O_3, the c/a ratio remains almost constant with applied pressure and, for Fe_2O_3, this ratio varies only slightly; it is found that the a-axis in V_2O_3 is almost three times more compressible than its c-axis. They also pointed out that the oxygen positions in the V_2O_3 unit cell approach an ideal HCP arrangement with increasing pressure.

The lattice in V_2O_3 has some puzzling changes as a function of temperature. The most general effects are observed in the behavior of the thermal expansion coefficients of V_2O_3. These were obtained (*16*) by fitting the positions of diffraction peaks as a function of temperature to straight lines. Approximate values obtained for the thermal coefficients along the c-axis and in the basal plane, respectively, were $\alpha_c = -8.5$ ($\times 10^{-6}$) K^{-1} and $\alpha_a = 20$ ($\times 10^{-6}$) K^{-1}. Further, these values vary as a function of temperature (*49*). At room temperature, the anisotropy is readily apparent. As T is increased, α_a decreases and is 50% lower at 500 K than at room temperature whereas α_c increases changing its sign between 300 and 500 K. Increasing T past 500 K reverses the trend slightly. At 800 K, $\alpha_a = 13 \times 10^{-6}$ K^{-1} and $\alpha_c = 1.5 \times 10^{-6}$ K^{-1}. It is seen that the thermal expansion coefficients in the M′ phase are far more isotropic than in the M phase.

The crystallography of V_2O_3 was of great interest in determining the driving mechanism of these transitions. In particular, the Mott transition would require (*50*) that the relevant metal–metal distances in the AFI phase should be larger and, in fact, this was found to be true.

With X-ray diffraction techniques it was determined (*14*, *19*) that, at the transition to the AFI phase, the trigonal unit cell having $R3c$ symmetry undergoes a monoclinic distortion with $I2/a$ spacegroup describing the unit cell. However, if one ignores the change in symmetry, it is seen that, as the system goes from M to AFI, the c-axis contracts

and the *a*-axis expands. In spite of the fact that the *c*-axis in the AFI state is approximately 5% smaller than in the M phase, the metal–metal distance along the *c*-direction is actually about 5% larger. V–V distances in adjacent *c*–*a* planes remain largely unchanged. Together with the magnetic structure, this means that V–V distances with parallel spins increase while those with antiparallel spins show no substantial change. All V–O distances are maintained at an approximately constant value. Significant changes occur in the V–V distances and it is assumed that the O–O distances vary mainly to accommodate the changes in the lattice, allowing the V–V distances to vary while keeping the V–O spacings constant. As *T* is increased, the V–V distances are seen to go through a minimum at about 530 K where the M′ phase sets in.

Corresponding to the lattice change at the M–AFI transition, there is also an enormous change in volume; the cell volume of the AFI phase is about 3.5% larger than that of the M phase. This large change in the volume causes samples to crack up severely on cycling through the M–AFI transition.

In Cr-doped specimens, the M, I, and M′ phases are all trigonal. In samples where the AFI–M transformation occurs, the lattice changes parallel those in pure V_2O_3 and the lattice parameters are also very similar (*51*) to the M phase in the undoped material. The changes at the M–I transition involve a compression of the *c*-axis and an expansion of the *a*-axis rather like the M–AFI change but without a reduction in symmetry. The volume of the I phase is also similar to that of the AFI phase, greater than the volume of the M state by about 1.5%. Hence in samples where the transition to the I phase occurs directly from the AFI state, the problem of sample cracking is no longer as severe since the change in unit cell volume is not as drastic as at the AFI–M change. For samples that bypass the M phase, both the *a* and the *c* lattice parameters increase smoothly (*25*) as *T* is raised, indicating only a thermal expansion that appears to be roughly constant with temperature. The thermal expansion coefficients in the I phase of the Cr-doped material are much smaller than for samples in the M phase and are also considerably more isotropic.

Oddly enough, the distances between the V atoms in the M′ and I phases is more closely related to the V–V spacing in the AFI phase, rather than the M phase, even though the symmetry of the M′ phase, like that of the M state, is trigonal. Once again, the M phase is unique in its large *c*/*a* ratio, its larger *c*-axis, but smaller V–V distances along the *c*-axis. From these accounts, the M′ and I phases of these materials are apparently very similar, showing only a difference in the resistivity.

In the M phase in the Cr-doped materials, careful crystallographic studies (*25*) indicate a large temperature range where both the M and I phases coexist, in spite of the sharpness in the resistivity discontinuity exhibited at the M–I transition. As previously noted, this explains the rise in resistivity of the M phase as the Cr content is increased, since it is pointed out that quite a small fraction of the M phase can drastically reduce the resistivity. In Ti-doped and O-rich V_2O_3 samples, both the metallic phase and insulating phase, where it exists, emulate their counterparts in the pure compound.

At M–AFI, each of the (hexagonally indexed) 110 axes in the trigonal cell becomes a unique 010 axis in the monoclinic cell. The change from trigonal to monoclinic is accomplished by the rotation of V–V pairs in the *c*–*a* plane by approximately 1.8°. Since this tilting can occur about anyone of the three equivalent *a*-axes in the trigonal cell, a triple twinning of all reflections with a non-zero *l* component occurs. This distortion can be visually seen as the metal atoms moving in a direction approximately perpendicular to the *c*-axis as shown in Fig. 4.

The reduction of symmetry from trigonal

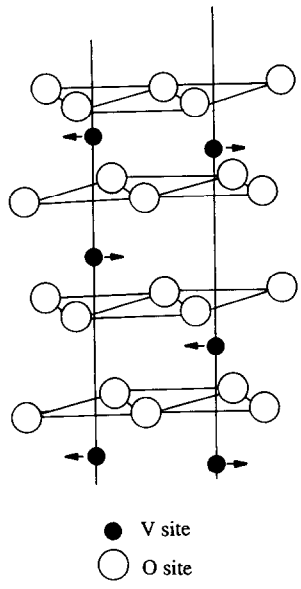

FIG. 4. A schematic view of the V_2O_3 lattice. The vertical lines point along the c-axis and sheets of oxygen atoms lie in the basal plane. At the transition to the AFI phase, the V atoms move as indicated by arrows; the V–V pairs may be visualized as rotating about the c-axis by 1.8°. (From Ref. (*19*).)

to monoclinic was studied in some detail in pure and Cr-doped V_2O_3; this change was monitored by the triple twinning of $(006)_H$ reflection. The domains are reported to be approximately equipartitioned, at least in the large samples used in neutron scattering studies (*52–54*). For the M–AFI transition, this splitting appears at T_{M-AFI} and there is little or no change as the temperature is decreased. In $(Cr_xV_{1-x})_2O_3$, for $x = 0.03$, this twinning is again observed at the onset of the AFI phase. However, lowering the temperature, from 150 to 130 K, is seen to increase the distortion, as seen by the separation between the three peaks. This is rather reminiscent of a magnetostrictive effect, where the increase in magnetization on lowering the temperature also increases the distortion. Further, for Cr content, $x = 0.06$, there is no longer any clearly defined triple twinning. It is possible, although unlikely, that a single domain dominates since there is some broadening of the peak, but, as shown in Fig. 5, there is no intensity where such peaks from a twin in the 3% (or pure) sample is observed. This is qualitatively in agreement with older studies (*55*) that showed that although the monoclinic structure exists for $x \leq 0.25$, the distortion is reduced for $x \geq 10\%$.

In addition, a high resolution γ-ray study (*54, 56*) of a single magnetic domain in 3% $Cr\text{-}V_2O_3$ shows that there are crystallographic precursors to the magnetic transition. That is to say, these effects occur a few degrees prior to the onset of magnetic order. These changes are smaller but of the same order as the monoclinic distortion. In the doped samples, we begin to get a hint that, perhaps, the magnetic, structural, and electrical transitions do not occur simultaneously.

These changes in the crystal structure are bound to be reflected in the lattice dynamics. In order to study the contribution of the lattice dynamics to the transitions, ultrasound and neutron scattering experiments were conducted on pure and Cr-doped V_2O_3. In most cases, unfortunately, mea-

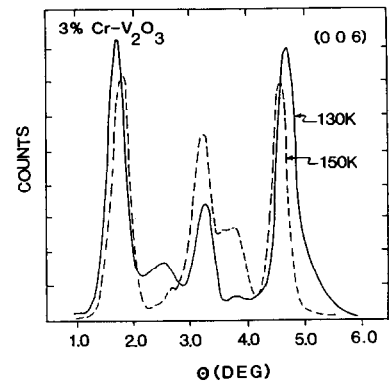

FIG. 5. The $(0\ 0\ 6)_H$ reflection in 3% $Cr\text{-}V_2O_3$ at 150 and 130 K. The splitting of the peaks can be seen to increase significantly as the temperature is lowered by just 20 K, suggesting a magnetostrictive mechanism for the crystal structure distortion. (From Ref. (*53*).)

surements were not made in the AFI phase because sample fracture problems plague the ultrasound work and the inherent multidomain nature of the AFI phase complicates neutron scattering measurements. Nevertheless, the data obtained in the other phases as a function of temperature and doping indicate some very puzzling features.

In pure V_2O_3, ultrasound measurements (*57, 58*) of force constants C_{11} and C_{12} show a strong minimum and C_{33} and C_{13} show a somewhat more shallow dip at $T \sim 530$ K, where the system goes from M to M′ with increasing temperature. C_{12}, in fact, becomes negative between 500 and 570 K. Reports conflict as to the recovery of the softening in the C_{11} and C_{33} force constants, but the behavior for $T < 530$ K is in good agreement. One of these reports show that the data is consistent with the existence of a small percentage of a second phase. The force constant along the other direction, C_{44}, begins to decrease with T somewhat, even at 300 K; this is seen as being indicative of a phase transition with a crystallographic component at lower temperature, as it has been shown (*59, 60*) that for a trigonal lattice to be stable, C_{44} must be non-zero.

In the I phase in Cr-doped V_2O_3, the value of C_{44} decreases monotonically (*61, 62*) with temperature. Ultrasonic work was hampered due to the formation of microcracks at the I–M transition, but neutron scattering measurements (*54, 55*) verified the softening of C_{44} in the I phase and found, in addition, that the onset of the M phase stabilized C_{44} at its value just prior to the I–M phase change. Strangely, in samples where no M phase is encountered, C_{44} softens completely to zero. This total softening coincides with the I–AFI transition. This is not unexpected since C_{44} must be greater than zero for the stability of the trigonal structure. It should be mentioned here that the entire dispersion curve does not soften with decreasing temperature; the softening is only observed at small q close to the zone center. The cause of this softening is undetermined.

Other features in the phonon dispersion measurements (*54, 55*) include the fact that all measured modes are stiffer in both the M′ and M phases compared to the I phase in the Cr-doped specimens. Raman scattering measurements (*63*) agree that, for modes measured, phonons are stiffer in the *M* phase. The fact that the M′ modes are stiffer than the I modes, despite the higher temperatures, is the first indication that the M′ and I phases are distinct, beyond just the resistivity difference. Neutron scattering results (*55, 62*) also indicate a transverse mode that is not identified, in addition to the expected transverse and longitudinal phonon modes. This extra mode appears in the M phase in pure V_2O_3 as well as in the M′ phase in 1.5% CrV_2O_3. In the 1.5% Cr-doped sample, the intensity of this branch is observed to be greatly reduced as the sample enters the I phase with decreasing temperature. That the unidentified transverse $(h,h,0)$ mode is not seen in the M phase in Cr-doped samples may be due to the coexistence of two phases in this region. As has been pointed out, the "M" phase in Cr-doped samples may contain quite a small fraction of the M phase. This would lead to a proportionally smaller intensity to the modes characteristic of the M phase. If this is the case, then this mode may be common to the M′ and M phases.

Ultrasonic measurements (*64*) of sound velocities in Cr-doped samples that undergo the I–M phase change under applied pressure show linear pressure dependences, changing by $\sim 1\%$ for an applied pressure of 4 kbar. It is interesting to note that the bulk modulus of 3% Cr-V_2O_3 decreases with pressure, considered to be possibly a precursor to the volume collapse at I–M. The bulk modulus for the pure material increases with applied pressure.

As in superconductivity, observation of the isotope effect will indicate the relative importance of the lattice to the transitions.

Measurements of the effect of substituting ^{16}O with ^{18}O were reported. Enrichment by ^{18}O had effects on all the transitions in both pure and 1% Cr-V_2O_3. In pure V_2O_3, replacing 11 at.% of ^{16}O by ^{18}O resulted (*65*) in increasing the transition temperature of the M–AFI change by 2.3 K from 157 K. In 1% Cr-V_2O_3, 19 at.% of ^{18}O was observed (*66*) to result in raising the M–AFI transition temperature by approximately 3 K and lowering the M–I phase change by almost 9 K. This was interpreted as being due to the lattice contribution, proportional to $\delta M/M^2$, to the free energy in the M phase; the effects on the AFI and I phases were ignored.

It is clear that the lattice structure and dynamics play a significant role in these phase transformations. The large hysterisis associated with all the changes also points to the lattice playing a dominant role. However, it is also clear that there are other interactions that contribute to the features of this phase diagram.

(*c*) *Magnetic Properties*

Magnetic order at low temperatures is the most stable feature of the V_2O_3 system and occurs in all compounds that undergo a metal–insulator transition. The AFI phase was conclusively determined by Moon (*15, 20*) to be antiferromagnetic using neutron spin-flip scattering techniques. The magnetic structure of V_2O_3 is unique among transition metal oxides, however. A magnetic moment of 1.2 μ_B per V atom is observed as the saturation value. The moments lie 71° from the *c*-axis and perpendicular to the *a*-axis, again using pseudo-hexagonal axes and alternate layers along the $(110)_H$ are stacked antiferromagnetically. The space group of the AFI cell was determined to be $I2/a$. There is a more recent publication that reports (*52*) the observation of the $(3/2,3/2,3)_H$, which makes the structure inconsistent with the $I2/a$ symmetry. However, this is a minor issue; the same authors verify the moment of $\sim 1.2\ \mu_B$. In this context, it is interesting to note that Moon has suggested (*20*) the existence of a component of the moment that is effectively a tilt out of the ferromagnetic plane, which would (*67*) also violate the $I2/a$ symmetry, even though crystallographically the $I2/a$ space group is still valid.

In pure V_2O_3, the magnetic transition outlined above is first-order and the magnetic intensity reaches about 90% of its saturation value (*52*) almost instantaneously. As T is lowered further below $T_{M\text{–}AFI}$, the magnetic intensity increases only gradually. When the magnetization curve for T just below $T_{M\text{–}AFI}$ is extrapolated, different authors report second order Néel temperatures of 220 (*68, 69*) and 290 K (*20*), respectively. That the Neel temperature is some 100 K above $T_{M\text{–}AFI}$ suggests that the onset of the metallic behavior prematurely disrupts the magnetic order. As previously noted, whatever interactions drive the system to become metallic shorten the V–V distance; perhaps it is also the cause of the disruption of the AFI phase. This first-order onset of magnetic long range order is seen in all samples that undergo the M–AFI transformation. There is about 10 K hysterisis at this transition.

In contrast, in chromium-doped samples (*54, 55, 70*) for which the transition to the AFI occurs directly from the I phase, the magnetization sets in more gradually. For 3% doping fitting the measured magnetic intensity to a power law, $I \propto (T_{M\text{–}AFI} - T)^{2\beta}$, indicates a value for the critical exponent β of the order parameter of 0.19. This rather low value is attributed to the system being close to a higher order critical point. For comparison, $\beta \simeq -1/3$ for a 3-D Heisenberg system. For 6% Cr-V_2O_3, the value of β obtained was only slightly larger, but the straight line fit for the 6% Cr-V_2O_3 specimen was valid over a larger range below the critical temperature than for 3% Cr-V_2O_3. The hysteresis at this transition is also much smaller. If this trend continues it is to be expected that the transition would become

second-order for larger amounts of Cr. Moreover, as increasing Cr content moves the system further from the M phase the eventual result should be a quite ordinary second-order magnetic transition.

Neutron scattering measurements (*43, 55, 70*) have measured the spin wave band gap in pure and Cr-V_2O_3. The energy of the gap is found to be 4.75 meV for pure V_2O_3 at T_{M-AFI} and there is no change as the temperature is lowered. This is also true for Cr-doped specimens that undergo a first-order onset of magnetic order. However, in 3% Cr-V_2O_3, the spin-wave band gap is observed to be much reduced at T_{I-AFI} and is ~2.9 meV at $T = 175$ K, increasing to a saturated value of ~4.75 meV at $T = 55$ K, very approximately following the magnetization curve. This suggests that, at the lowest temperatures, the spin dynamics of pure and 3% Cr-V_2O_3 is identical. The spin wave gap does not decrease completely to zero at T_{I-AFI}; perhaps all this indicates is that the I–AFI transition in 3% Cr-V_2O_3 is still weakly first-order, as is the resistivity.

The first observations that suggested antiferromagnetism was a sharp rise (*71*) in the magnetic susceptibility, χ, at the transition temperature, T_{M-AFI}. Measurements (*72, 73*) of χ in the M, M′, and I phases give some idea of the differences in the magnetic interactions of these three phases. In the range $160\ K \leq T \leq 400\ K$, χ obeys a Curie–Weiss law with $\theta = -600$ K and $\mu \simeq 2.37\ \mu_B$. This is anomalous behavior for a metal, but it has been shown (*74*) that this a near singularity in the density of states at the Fermi energy could give rise to a Curie–Weiss regime. A small but definite difference seen in diffuse neutron scattering measurements is also consistent with paramagnetic behavior in the M phase. For $500 < T < 650$ K, a second Curie–Weiss region exists; the only difference is a small difference in the effective moment ($\mu \simeq 2.69\ \mu_B$) for the M′ phase. Careful measurements also show a small peak at $T = 518$ K. At this temperature, Parette and Madhav Rao (*75*) report a peak in the diffuse neutron scattering, as a function of temperature, at low q-values. This is approximately a 20% effect and is attributed to "superparamagnetic clusters" with a radius of 300 Å.

In $(Cr_xV_{1-x})_2O_3$ samples that undergo the M–I transformation, χ exhibits (*73*) either a broad maximum or a broad plateau at a temperature which is identified, by extrapolation, as the second-order Neel temperature. Again, in general, ordered magnetism disappears before this temperature is reached. As the Cr content is increased, the Curie–Weiss temperature changes sharply (*76*) from $\Theta = -600$ K for $x = 0$ to $\Theta = -350$ K for $x = 0.02$. For larger values of x up to 0.20, Θ does not appear to change further. The temperature of the magnetic transition rises on the addition of Cr up to 3% and then gradually decreases for additional dopant amounts; in parallel with the resistivity change.

Most of the previous observations suggest that the crystallographic, magnetic, and electrical transitions are simultaneous. The strongest experimental observation (*52*) against a direct link between the metal–insulator transition and long-range magnetic order is reported for O-rich $V_2O_{3+\delta}$, $\delta = 0.0198$, where the two effects manifest themselves at different temperatures. It is reported that, in this sample, the M–AFI transition occurs at ~50 K. However, long-range magnetic order sets in almost 40 K above T_{M-AFI}, although the ordered moment in the M phase, 0.9 μ_B, is smaller than the 1.2 μ_B for the AFI phase. It is always possible that the sample inhomogenieties caused this. However, it seems unlikely that inhomogeneous samples could cause the behavior shown in Fig. 6, since the dependence of the magnetization on heating and cooling is distinctly different, beyond simply a large hysteretic effect. This result has not drawn much comment in the literature and could play a significant role in unraveling the tran-

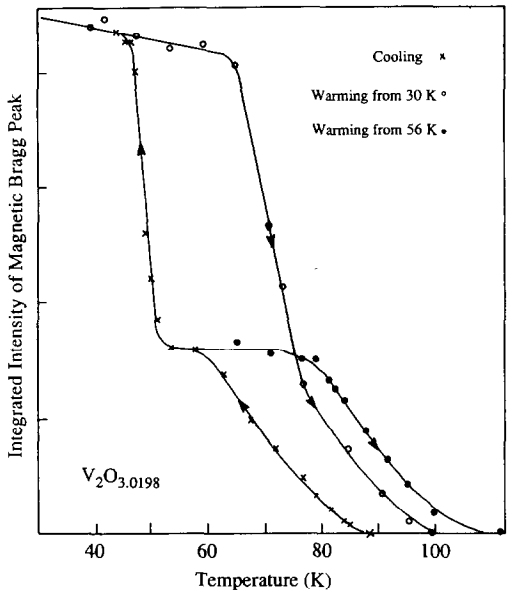

FIG. 6. The magnetic intensity as a function of temperature for cooling and warming cycles in $V_2O_{3.0198}$. The crystallographic transformation in this sample occurs at approximately 50 K. Still, there is magnetic intensity at 90 K. (From Ref. (*52*).)

sition mechanisms. It would, for instance, be interesting to find out whether magnetism occurs as a function only of metal–metal distances, independently of phase.

A number of NMR studies provided the first definite clues to the presence of magnetic order in the AFI phase. The first observation of the disappearance of the NMR signal below T_{M-AFI} indicating antiferromagnetic behavior was by Jones (*72*) in 1964. In addition, authors of various NMR reports (*73, 74, 77*) are in agreement that the Knight shift data obtained from Cr-doped V_2O_3 unmmistakably indicates the coexistence of two phases in what is generally referred to as the 'M' phase in Cr-V_2O_3. Also, the intensity of the NMR signal corresponding to the I phase grows at the expense of the M phase signal as either temperature or Cr content is increased, that is, with the approach of the I phase in resistivity data. This coexistence of the NMR signal due to M and I phases may indicate only a local disposition of the metal ions and not necessarily clustering. However, crystallographic observations of a splitting of the Bragg peak positions detailed in the previous section suggest some degree of clustering of each of these phases in the sample. In addition, the pressure-dependence studies of the Knight shift, when analyzed in terms of spin and Van Vleck components, are seen as indicators that the M phase in pure V_2O_3 is very close to a transformation to a paramagnetic insulating phase.

This proximity of the M phase to an insulating phase at room temperature becomes important in a scenario where it is thought that the M phase actually transforms to the I phase briefly, at which time the AFI phase overcomes the I phase.

(*d*) *Electron Band and Other Properties*

Although detailed band structure discussions are beyond the scope of this work, there are a number of significant measurements that deserve mention. Optical properties of V_2O_3 include a band with the maximum at approximately 1.1 eV and the authors (*78*) attribute the onset of the M phase due to the collapse of E_g. They report a band at 1.7 eV which decreases in width and intensity at the AFI transition. Increased intensity in the M phase is interpreted as an indication of a greater degree of hybridization in this phase.

Photoelectron spectroscopy (*79, 80*) indicates that the 3*d* band shifts to slightly higher energy as the material transforms from AFI to M and that there is a significant rise in the intensity of this signal. A plasmon peak is also seen in the M phase. Further, the 3*d* band broadens and shifts to higher energies at 600 K. X-ray absorption near edge spectra (XANES) are consistent (*81*) with the metal ions in V_2O_3 being in a V^{3+} state, as would be expected from the oxidation state.

Muon spin resonance studies (*68, 69, 82*) indicate that modifications in the itinerant band states are small on going through the M–AFI transformation. The identification of the sites where the muons are stable are indicative of V–V pairing. The magnetization curve was also determined by this method with an extrapolated Néel temperature of 220 K.

Recent resonant photoemission studies (*83, 84*) of the V_2O_3 system have been reported. These studies indicate that there are no major differences in the electronic band structure between pure and Cr-doped materials. It would appear that the difference in the resistance properties of the M and I states are not reflected in the band structure. This may indicate that the two phases are electronically very close to each other. Also notably, there is no clear-cut gap between the O^{2p} and V^{3d} electronic states. The data are consistent with a combination of effects due both to molecular orbitals, with lobes of charge pointing along the *c*-axis, as well as due to delocalized *d*-bands. As would be expected, the *d*-bands are reported to be close to the Fermi energy. Unfortunately, these measurements have not been extended to the AFI phase.

Discussion and Conclusion

Various theories have been proposed to explain the experimental data. The most detailed treatment is that Weger and collaborators (*9*) who reason that the change in the a_1 states from a band description to a localized one is reflected by a change in the distance between the V atoms. A large number of experimental facts can be explained in this framework. A model (*85*) including a combination of localized electrons and a Fermi fluid can also model the gross features of the data. A charge density wave model of this transition was proposed (*86*). However, satellites to the Bragg peak seen by Sinclair and Colella (*87*) have not been verified in later experiments (*88, 89*). Theoretical work is still in progress.

The salient experimental features are outlined here. The antiferromagnetic order in the AFI phase is definitely the most stable feature of the vanadium sesquioxide phase diagram and, in itself, it is not unreasonable that this transition metal oxide should order magnetically at lower temperatures. Neither is it unreasonable that the system should undergo a second-order transition to a nonmagnetic phase with rising temperature. The structural trigonal-monoclinic transformation would appear to be magnetostrictive in origin.

The metallic M phase is, however, unexpected. It is most likely that the M phase is in fact semimetallic rather than metallic and has some rather unusual properties: The electronic contribution to the specific heat is anomalously large, and the pressure-stabilized M phase shows a large T^2 dependence in the resistivity up to 100 K and has a Curie-Weiss susceptibility. These anomalies have been addressed in the theoretical treatment by Hertel and Appel (*36*) in a Fermi liquid model involving antiferromagnetic spin fluctuations caused by the exchange of localized A_{1g} electrons between two V_2 pairs along the *c*-axis. They concluded that the metal–insulator transition is a magnetic transition driven by the exchange interaction between the E_g electrons. However, although the onset of the M state seems to disrupt the magnetic order in most cases, the results of Yelon *et al.* (*52*) indicate that this may not always be true.

Various measurements indicate the M phase being rather close to a transformation to a paramagnetic insulating phase. The analysis of the pressure-dependent Knight shift has been interpreted to indicate this in the case of a previous review. In addition, the resonant photoemission data show that the electronic band structure does not differ very much between the I and M phases. This is perhaps the strongest indicator that the M

phase is not far from being an insulator even at room temperature. If the band structure does not play a dominant role in the I–M change, the importance of spin fluctuation as well as that of the lattice cannot be ignored. The large hysterisis at these transitions as well as the existence of an isotope effect point toward the lattice contributions to these phase changes. These features need to be addressed theoretically.

The I and M′ phases, on the other hand, seem very similar and a claim could be made that the two are more or less the same; the difference in resistivity can be explained by the fact that the temperature of this phase change is approximately equal to the activation energy in the AFI regime. However, the lattice is clearly different. All of the lattice modes measured in the M′ phase are either stiffer or the same as in the I phase, in spite of the higher temperature. In fact, in terms of the lattice dynamics, the M′ phase seems to be more closely related to the M phase. This can be interpreted as evidence that the three (M, I, and M′) phases are distinct.

It is not known what interactions cause the trigonal structure of the I phase to become unstable and shear as the temperature is decreased, but, given this softness of the lattice, it appears as though the structural transformation is caused by magnetostriction. This is consistent with the observation of the increasing distortion as the temperature is lowered in the non-first order transitions. The question then arises as to why the M–AFI change is accompanied by a lattice distortion. It has been proposed that the M phase, being reasonably close to an insulator already, transforms momentarily to the I phase. Here, since the temperature is lower than $T_{\text{I–AFI}}$, the effects are more catastrophic. In addition, since the extrapolation of the magnetization in the AFI state, prior to the M phase onset, yields Néel temperatures rather higher than $T_{\text{M–AFI}}$, the magnetization would be well developed by this temperature.

It appears then that the metallic phase interrupts the continuation of antiferromagnetic behavior in most cases. The observed magnetic ordering in the M phase in O-rich V_2O_3 is an exception. But even in this case, the structural transformation is coincident with the metal–insulator change. Hence, in the scheme above, the metal–insulator transition occurs along with its concomitant lattice instability in the I phase and results in the transformation of the crystal symmetry.

Further, the monoclinic distortion is brought about by the V atoms moving in a direction approximately perpendicular to the c-axis, the same direction in which the lattice is unstable to shear. Since C_{44} is not soft in pure V_2O_3, there is no apparent reason for the monoclinic shear distortion in the pure compound to resemble the change of the 3% Cr-doped sample so closely. This may be more evidence in favor of the short-lived M–I transformation, prior to the onset of the AFI phase.

The body of experimental work is significantly larger for the Cr-doped as compared to the Ti-doped or O-rich regions of the phase diagram and it is not clear why the M–AFI transition is suppressed in the latter compounds. It is possible that the major effect of nonstoichiometry (in O-rich samples) or of doping (in samples with Ti) is merely to dilute the spin interactions between the V atoms; somehow this results in the prolonged stability of the metallic phase. In any event, it is obvious that the system is complicated.

There is some confusion in the literature as to which of the two, M–AFI or M–I, transformations was thought to be a Mott transition. Perhaps this is due to the fact that both of them have been candidates for the Mott interpretation at various times by various groups. The data would seem to indicate that the AFI–M change is much more complex than a simple Mott transition. For instance, there are crystallographic precursors to the AFI transition in 3% Cr-V_2O_3,

the distortion appears to be magnetostrictive, and finally, there is a case where all the three (crystallographic, electrical, and magnetic) components of the transition do not appear simultaneously. It is obvious that there is a delicate balance between magnetic, structural, dynamic, and electronic components in the system that will not lend itself to simple explanations.

In conclusion, it is readily apparent that the goings-on in pure and doped vanadium sesquioxide have been studied experimentally in great depth and, undoubtedly, this will continue till the puzzle is solved. It is likely that many nuances of phase transition mechanisms in the field of solid-state physics will be better understood when V_2O_3 is fully explained.

References

1. Review articles (also see references therein): J. M. Honig, *J. Solid State Chem.* **45,** 1 (1982); J. M. Honig and L. L. Van Zandt, *Annu. Rev. Mater. Sci.* **5,** 225 (1975); D. B. McWhan, T. M. Rice, and J. P. Remeika, *Colloq. Int. C. N. R. S.* **188,** 149 (1970); T. M. Rice and D. B. McWhan, *IBM J. Res. Dev.* **14,** 251 (1970).
2. M. Foex, *C.R. Acad. Sci.* **223,** 1126 (1946); **229,** 880 (1949).
3. N. F. Mott, *Proc. Phys. Soc. A* **62,** 416 (1949).
4. D. B. McWhan and T. M. Rice, *Phys. Rev. Lett.* **22,** 887 (1969).
5. A. J. MacMillan, "Laboratory for Insulation Research, Massachussetts Institute of Technology, Technical Report No. 172, October 1962."
6. D. B. McWhan, A. Menth, and J. P. Remeika, *J. Phys. (Paris) C* **32**(1), 1079 (1971).
7. F. J. Morin, *Phys. Rev. Lett.* **3,** 34 (1959).
8. J. Jaffray and R. Lyand, *Compt. Rend.* **233,** 133 (1951).
9. I. Nebenzahl and M. Weger, *Phys. Rev.* **184,** 936 (1969); M. Weger, *Philos. Mag.* **24,** 1095 (1971).
10. D. Adler, J. Feinleib, H. Brooks, and W. Paul, *Phys. Rev.* **155,** 851 (1967); D. Adler and H. Brooks, *Phys. Rev.* **155,** 826 (1967).
11. N. F. Mott, *Rev. Mod. Phys.* **40,** 677 (1968).
12. C. N. R. Rao and K. J. Rao, "Phase Transitions in Solids," McGraw-Hill, New York (1971).

12a. J. M. Honig and J. Spalek, *Proc. Indian Natl. Sci. Acad. Part A: Phys. Sci.* **52**(1), 232 (1986).

13. D. B. McWhan, T. M. Rice, and J. P. Remeika, *Phys. Rev. Lett.* **23,** 1384 (1969).
14. P. D. Dernier, *J. Phys. Chem. Solids* **31,** 2569 (1970).
15. R. M. Moon, *J. Appl. Phys.* **41,** 883 (1970).
16. D. B. McWhan and J. P. Remeika, *Phys. Rev. B* **2,** 3734 (1970) and references therein.
17. A. P. B. Sinha, G. V. Chandrasekhar, and J. M. Honig, *J. Solid State Chem.* **12,** 402 (1974).
18. H. Kuwamoto, J. M. Honig, and J. Appel, *Phys. Rev. B* **22,** 2626 (1980) and references therein.
19. P. D. Dernier and M. Marezio, *Phys. Rev. B* **2,** 3771 (1970).
20. R. M. Moon, *Phys. Rev. Lett.* **25,** 527 (1970).
21. E. D. Jones, *J. Phys. Soc. Japan* **20,** 1292 (1965).
22. K. Kosuge and S. Kachi, *J. Phys. Soc. Japan* **20,** 627 (1965).
23. T. Shinjo and K. Kosuge, *J. Phys. Soc. Japan* **21,** 2622 (1966).
24. A. Paoletti and S. J. Pickart, *J. Chem. Phys.* **32,** 308 (1960).
25. A. Jayaraman, D. B. McWhan, J. P. Remeika, and P. D. Dernier, *Phys. Rev. B* **2,** 3751 (1970).
26. D. B. McWhan, A. Jayaraman, J. P. Remeika, and T. M. Rice, *Phys. Rev. Lett.* **34,** 547 (1975).
27. J. M. Honig, G. V. Chandrasekhar, and A. P. B. Sinha, *Phys. Rev. Lett.* **32,** 13 (1974).
28. H. Kuwamoto, H. V. Keer, J. E. Keem, S. A. Shivashankar, L. L. Van Zandt, and J. M. Honig, *J. Phys.* **37,** C4–35 (1976).
29. D. B. McWhan, A. Menth, J. P. Remeika, W. F. Brinkman, and T. M. Rice, *Phys. Rev. B* **7,** 1920 (1973).
30. S. A. Shivashankar and J. M. Honig, *Phys. Rev. B* **28,** 5695 (1983) and references therein.
31. H. Kuwamoto and J. M. Honig, *J. Solid State Chem.* **32,** 335 (1980) and references therein.
32. Y. Ueda, K. Kosuge, and S. Kachi, *J. Solid State Chem.* **31,** 171 (1980).
33. J. M. Honig, personal communication (1980).
34. N. Otsuka, H. Sato, G. L. Liedl, and J. M. Honig, *J. Solid State Chem.* **44,** 230 (1982).
35. Resistance properties have been extensively examined. Results are in general agreement with those cited here.
36. P. Hertel and J. Appel, *Phys. Rev. B* **33,** 2098 (1986).
37. V. N. Novikov, B. A. Tallerchik, E. I. Gindin, and V. G. Prokhvatilov, *Sov. Phys. Solid State* **12,** 2061 (1971).
38. M. S. Kozyreva, V. N. Novikov, and B. A. Tallerchik, *Sov. Phys. Solid State* **14,** 639 (1972).
39. V. A. Perelyaev, G. P. Shveikin, and G. V. Bazuev, *Tr. Inst. Khim. Ural. Nauch. Tsentr. Akad. Nauk. SSSR* **25,** 8 (1971).

40. Y. UEDA, K. KOSUGE, S. KACHI, AND T. TAKADA, *J. Phys. (Paris) Colloq.* **40,** C2–275 (1979).
41. D. B. MCWHAN, J. P. REMEIKA, T. M. RICE, W. F. BRINKMAN, J. P. MAITA, AND A. MENTH, *Phys. Rev. Lett.* **27,** 941 (1971).
42. J. M. HONIG, H. V. KEER, G. M. JOSHI, AND S. A. SHIVASHANKAR, *Bull. Mater. Sci. (India)* **3(2),** 141 (1981).
43. W. B. YELON, S. A. WERNER, R. E. WORD, J. M. HONIG, AND S. A. SHIVASHANKAR, *Phys. Rev. B* **24,** 1818 (1980).
44. G. M. JOSHI, H. V. KEER, AND J. M. HONIG, *Int. J. Thermophys.* **1,** 185 (1980).
45. J. M. D. COEY, *Physica B* **91,** 59 (1977).
46. K. KOSUGE, *J. Phys. Chem. Solids* **28,** 1613 (1967).
47. L. W. FINGER AND R. M. HAZEN, *J. Appl. Phys.* **51,** 5362 (1980).
48. Y. SATO AND S. AKOMOTA, *J. Appl. Phys.* **50,** 5285 (1979).
49. T. BEGUEMSI, P. GARNIER, AND D. WEIGEL, *J. Solid State Chem.* **25,** 315 (1978).
50. N. F. MOTT, "Metal Insulator Transitions," Taylor & Francis, London (1974).
51. W. R. ROBINSON, *Acta Crystallogr. Sect. B* **31,** 1153 (1975).
52. W. B. YELON, S. A. WERNER, R. E. WORD, J. M. HONIG, AND S. A. SHIVASHANKAR, *J. Appl. Phys.* **52,** 2237 (1981).
53. M. YETHIRAJ, S. A. WERNER, W. B. YELON, AND J. M. HONIG, *Phys. Rev. B* **36,** 8675 (1987).
54. M. YETHIRAJ, S. A. WERNER, W. B. YELON, AND J. M. HONIG, *Physica B* **136,** 458 (1986).
55. A. F. REID, T. M. SABINE, AND D. A. WHEELER, *J. Solid State Chem.* **4,** 400 (1972).
56. J. R. SCHNEIDER, HMI-Berlin, personal communication (1984).
57. D. N. NICHOLS AND R. J. SLADEK, *Phys. Rev. B* **24,** 3155 (1981).
58. G. O. ANDRIANOV AND I. L. DRICHKO, *Sov. Phys. Solid State* **22,** 1619 (1981).
59. H. YANG AND R. J. SLADEK, *Phys. Rev. B* **32,** 6634 (1985).
60. R. W. TERHUNE, T. KUSHIDA, AND G. W. FORD, *Phys. Rev. B* **32,** 8416 (1985).
61. H. YANG, R. J. SLADEK, AND H. R. HARRISON, *Phys. Rev. B* **31,** 5417 (1985); *Solid State Commun.* **47,** 955 (1983).
62. M. YETHIRAJ, W. B. YELON, S. A. WERNER, AND J. M. HONIG, "AIP Conf. Proc. 89" (John Farber, Jr., Ed.), AIP, New York (1982).
63. C. TATSUTYAMA AND H. Y. FAN, *Phys. Rev. B* **21,** 2977 (1980).
64. D. N. NICHOLS, R. J. SLADEK, AND H. R. HARRISON, *Phys. Rev. B* **24,** 3025 (1981).
65. E. I. TERUKOV, W. REICHELT, M. WOLF, H. HEMSCHIK, AND H. OPPERMANN, *Phys. Status Solidi A* **48,** 377 (1978).
66. M. WOLF, E. I. TERUKOV, W. REICHELT, AND H. OPPERMANN, *Phys. Status Solidi A* **72,** 655 (1982).
67. B. VON LAAR, personal communication.
68. A. B. DENISON, C. BOEKEMA, R. L. LICHTI, K. C. CHAN, D. W. COOKE, R. H. HEFFNER, R. L. HUTSON, M. LEON, AND M. E. SCHILLACI, *J. Appl. Phys.* **57,** 3743 (1985).
69. Y. J. UEMERA, T. YAMAZAKI, Y. KITAOKA, M. TAGIGAWA, AND H. YASUOKA, *Hyperfine Interact.* **17–19,** 339 (1984).
70. M. YETHIRAJ, Ph.D. thesis (1985).
71. D. J. ARNOLD AND R. W. MIRES, *J. Chem. Phys.* **48,** 2231 (1968); M. GREENWOOD, R. W. MIRES, AND A. R. SMITH, *J. Chem. Phys.* **54,** 1417 (1971).
72. E. D. JONES, *Phys. Rev. A* **137,** 978 (1964).
73. A. C. GOSSARD, A. MENTH, W. W. WARREN, AND J. P. REMEIKA, *Phys. Rev. B* **3,** 3993 (1971).
74. M. RUBINSTEIN, *Phys. Rev. B* **2,** 4731 (1970).
75. G. PARETTE AND L. MADHAV RAO, *Solid State Commun.* **23,** 179 (1977).
76. A. MENTH AND J. P. REMEIKA, *Phys. Rev. B* **2,** 3756 (1970).
77. A. L. KERLIN, H. NAGASAWA, AND D. JEROME, *Solid State Commun.* **13,** 1125 (1973).
78. V. G. MOKEROV, I. V. RYABIBIN, AND G. B. GALIEV, *Sov. Phys. Solid State* **22,** 712 (1980).
79. S. VASUDEVAN, M. S. HEGDE, AND C. N. R. RAO, *Solid State Commun.* **27,** 131 (1978).
80. J. M. HONIG, L. L. VAN ZANDT, R. D. BOARD, AND H. E. WEAVER, *Phys. Rev. B* **6,** 1323 (1972).
81. J. WONG, F. W. LYTLE, R. P. MESSMER, AND D. H. MAYLOTTE, *Phys. Rev. B* **30,** 5596 (1984).
82. K. B. CHAN, R. C. LICHTI, C. BOEKEMA, A. B. DENISON, D.W. COOKE, AND M. E. SCHILLACI, *Hyperfine Interact.* **31,** 481 (1986).
83. K. E. SMITH AND V. E. HENRICH, *Solid State Commun.* **68,** 29 (1988).
84. K. E. SMITH AND V. E. HENRICH, *Phys. Rev. B* **38,** 5965 (1988-II): *Phys. Rev. B* **38,** 9571 (1988-I).
85. J. SPALEK, A. DATTA, AND J. M. HONIG, *Phys. Rev. B* **33,** 4891 (1986).
86. A. W. OVERHAUSER, personal communication (1981).
87. F. SINCLAIR AND R. COLELLA, *Solid State Commun.* **31,** 359 (1979).
88. M. YETHIRAJ AND A. C. LARSON, unpublished (1987).
89. J. M. HONIG, personal communication (1988).